Inorganic Chemistry

ARTICLE

pubs.acs.org/IC

Elaboration of Covalently Linked Polyoxometalates with Ruthenium and Pyrene Chromophores and Characteriation of Their Photophysical Properties

Benjamin Matt,[†] Christophe Coudret,[§] Christine Viala,[§] Damien Jouvenot,[∥] Frédérique Loiseau,[∥] Guillaume Izzet,[†,*] and Anna Proust[†,‡]

[†]Institut Parisien de Chimie Moléculaire, UMR CNRS 7201, UPMC Université Paris 06, 4 place Jussieu, 75252 Paris cedex 05, France

[‡]Institut Universitaire de France, 103 Bd Saint-Michel, 75005 Paris, France

[§]CEMES, 29 rue Jeanne Marvig, BP 94347, 31055 Toulouse, Cedex 4, France

[∥]Département Chimie Moléculaire, Université Joseph Fourier, CNRS UMR 5250, BP 53, 38041 Grenoble cedex 9, France

Supporting Information

ABSTRACT: Keggin and Dawson-type polyoxometalates (POMs) decorated by organometallic [cyclometalated ruthenium(II) polypyridine complex] or organic (pyrene) chromophores were prepared by postfunctionalization of hybrid disilylated POM platforms. The connection is made in a very efficient and modular way via Sonogashira coupling reactions, which provide a rigid linkage between the POM and the photoactive centers. Electronic properties have been inferred from electrochemical and photophysical studies and reflect poor electronic interactions between both partners. The presence of the POM leads to luminescence quenching of the chromophores, which was attributed to an intramolecular electron transfer from the chromophore to the POM. The rate of this process is much faster in the POM−pyrene than in the POM−Ru system. It depends on the driving force dictated by the redox potentials of both partners but also in the case of the POM−Ru system on the presence of the metallacycle, which acts as a molecular insulator and delays the intramolecular electron transfer. In the POM−Ru system, a comparative study of the luminescence quenching showed that the electron transfer is still more important in the covalently bonded hybrids than in systems where the POM and the ruthenium complexes are assembled via electrostatic interactions.

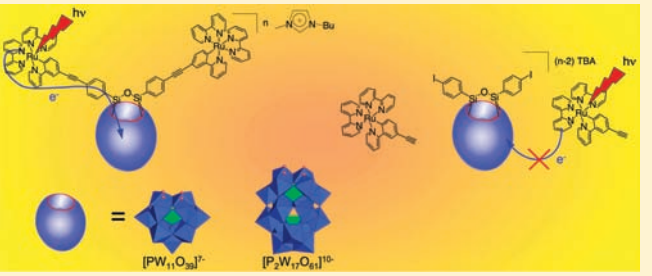

INTRODUCTION

Photoconversion of light into chemical fuels relies on photoinduced electronic charge separation with suitable lifetime to permit redox reactions with external substrates to proceed. The design of functional artificial photosynthetic devices requires these major scientific challenges to be overcome. Actually, charge photoaccumulation has rarely been described in the literature on homogeneous molecular system.[1,2] Furthermore, only few molecular electrocatalysts are able to compete with colloidal dispersions of noble metals for the hydrogen evolution reaction.[3−8] Most of these systems rely on the use of external sacrificial electron donors. To overcome this issue, a recent strategy was developed by anchoring a molecular photoactive system on nanocrystalline TiO_2.[9] In such a nanosystem, the absorption of two photons leads to accumulation of two holes on the chromophore and two electrons on the semiconductor in a nearly quantitative yield without the use of external donor. The research of a molecular architecture that could both perform multiple electron transfer and act as an efficient electrocatalysts is thus of high interest for its implementation in functional artificial photosynthetic devices. In search for such alternative materials, polyoxometalates (POMs) have recently attracted particular attention.[10,11] POMs are a unique family of molecular-scale oxide semiconductors with remarkably diverse structural and electronic properties.[12,13] These compounds have been widely used for the preparation of hybrid organic−inorganic materials and devices that might display advanced functions.[10,11] Many POMs are able to store several electrons under minor structural reorganization and their reduced forms display efficient electrocatalytical properties,[14] notably for the hydrogen evolution reaction.[15,16] As a consequence, POMs are attractive candidates for the development of functional artificial photosynthetic devices. Their association to a light-harvesting antenna is yet necessary, since POMs themselves are only photoactive in the UV part of the solar spectrum.[17−23] In most POM−dye materials reported in the literature, the

Received: April 29, 2011
Published: July 20, 2011

Scheme 1. General Synthetic Route to Photoactive POM-Based Hybrids[a]

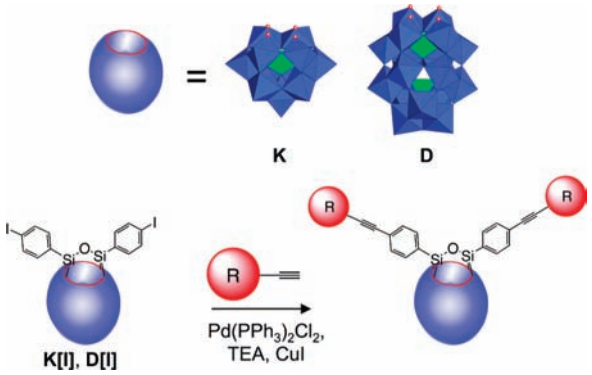

[a] K = $[PW_{11}O_{39}]^{7-}$, D = $[P_2W_{17}O_{61}]^{10-}$.

hybrid is assembled via electrostatic interactions.[24−29] These studies indicate strong interactions between the cationic and anionic moieties giving rise to charge transfer transitions between the cationic dye and the polyanion. Nevertheless, these systems suffer from a lack of structural and electronic control between both fragments. Fewer are examples of covalently attached dyes on POMs.[30−35] Despite elegant synthetic procedures developed for these tailor-made hybrids, the photophysical properties reported are still unsuitable for the development of photochemical devices aiming at photocumulative electron transfer. This can be attributed either to the absence of redox properties of the POM used in some systems[30,32] or to the important flexibility of the covalent linker between the POM and the chromophore.[33−35]

We recently developed a series of polyoxometalate-based platforms that can be efficiently postfunctionalized using classical organic reactions (Scheme 1).[36,37] Such methodology was applied to both redox active Keggin and Dawson series and we also described the Sonogashira coupling to pyrene units.

We herein extend the postfunctionalization of the platform to photoactive ruthenium complexes. The intention is to study the photoinduced electron transfer chemistry of the resulting hybrids following excitation of the chromophore. The high chemical versatility of the system offers several advantages. Chromophores and linkers can be easily chemically modified, while retaining a structural rigidity, which is crucial for controlling electron transfer. In the same way, the redox potential of the polyanion can be tuned in order to optimize the charge accumulation on the polyanion (see Scheme 2).

RESULTS AND DISCUSSION

Design of the Organometallic Synthon. Because of a unique combination of chemical stability, redox properties, and excited state lifetime, Ru(II) polypyridine complexes are good candidates for photochemistry devices[38−41] and are particularly adapted to study photoinduced electron transfers. A fundamental requirement is the stability of the oxidized and/or reduced forms, i.e., the reversibility of the oxidation and/or reduction processes in the ground state. Oxidation of Ru(II) polypyridine complexes usually involves a metal-centered orbital, with formation of genuine Ru(III) complexes, which are inert to ligand substitution. In a preliminary work we synthesized complex **1** (Scheme 3) according to a literature procedure,[42] with the intention to couple it with the POM−based hybrids **K**[**I**] and **D**[**I**], bearing iodo aryl moieties, thanks to a Sonogashira coupling reaction (Scheme 1).

The attempts of Sonogashira coupling between **1** and either **K**[**I**] or **D**[**I**] were performed following the conditions that we previously developed.[36,37] Unfortunately, in all cases no covalent adduct is observed, but electrostatic adducts between the ruthenium complex and the POMs are observed. In order to lower the electrostatic interaction between the POM and the ruthenium complex and to favor the C−C coupling reaction, we decided either to reduce the global ionic charge of the organometallic complex or to electronically enrich the terminal alkyne function. This prompted us to prepare the ruthenium cyclometalate complex **5**, which can be readily obtained from the available $[Ru(bpy)_2Cl_2]$ in four steps (Scheme 4). Cyclometalation of $[Ru(bpy)_2Cl_2]$ is assisted by dechlorination with a silver salt and proceeds readily on a large scale in boiling dichloromethane. As reported previously, the complex can very easily undergo an electrophilic bromination, which is regioselective for the para position.[43] The use of the mild brominating agent NBS in CH_3CN at room temperature scavenges the proton released that could destroy the compound. Once the halogen is introduced, the complex is a suitable synthon for Sonogashira ethynylation. The best acetylene-like synthon was the cheap, nonvolatile 2-methylbut-3-yn-2-ol, which allows a simple purification procedure by enhancing the chromatographic contrast with non-alcohol-containing compounds. Terminal alkyne deprotection in the classic conditions (Na in ^{i}PrOH) leads to complex destruction. We have found that the acetone cleavage could be quantitatively obtained in THF with a stoichiometric amount of ^{t}BuOK avoiding any protic solvents. The complex obtained following this procedure is a racemic mixture of the Λ and Δ enantiomers.

Coupling of the Organometallic Synthon to the POM. The coupling reaction between the cyclometalated ruthenium complex **5** and the hybrids bearing the iodoaryl moieties **TBA**−**K**[**I**] and **TBA**−**D**[**I**] occurs at 70 °C in 1 h under microwave activation, using $[Pd(PPh)_3Cl_2]$ and CuI as catalyst sources in DMF containing triethylamine (20 equiv). In order to get a total conversion of the starting POM, a slight excess of **5** (2.5 equiv) is needed, since the Glaser homocoupled product can be produced under these reaction conditions.[44] The resulting POM−ruthenium hybrids are consequently obtained as a mixed TBA and ruthenium cyclometalated salts. Because of strong electrostatic interactions between the POM−ruthenium hybrids and the ruthenium complexes, neither POM−ruthenium hybrid **K**[**Ru**] nor **D**-[**Ru**] could be isolated as a pure TBA salt, even after addition of a large excess of TBABr. Nevertheless, a metathesis reaction can be performed by solubilizing the crude hybrids in a DMSO/ionic liquid (1-butyl-3-methylimidazolium chloride)[45,46] mixture. After subsequent addition of EtOH, the POM−ruthenium hybrids precipitate and are recovered as imidazolium salts in good yields. **Im**−**K**[**Ru**] and **Im**−**D**[**Ru**] were characterized by ^{1}H and ^{31}P NMR spectrometry, FT-IR spectroscopy, UV−vis spectroscopy, elemental analysis, and electrochemistry. Both hybrids were subjected to ESI-MS, but this technique failed to give informative values for **Im**−**K**[**Ru**] because of its high m/z value (m/z = 4082). The ^{1}H and ^{31}P NMR spectra of **Im**−**K**[**Ru**] and **Im**−**D**[**Ru**] are those of unique species, although these compounds are mixtures of

dx.doi.org/10.1021/ic200906b |*Inorg. Chem.* 2011, 50, 7761–7768

Scheme 2. Molecular Drawing of the Four Photoactive POM-Based Hybrids Described in This Study[a]

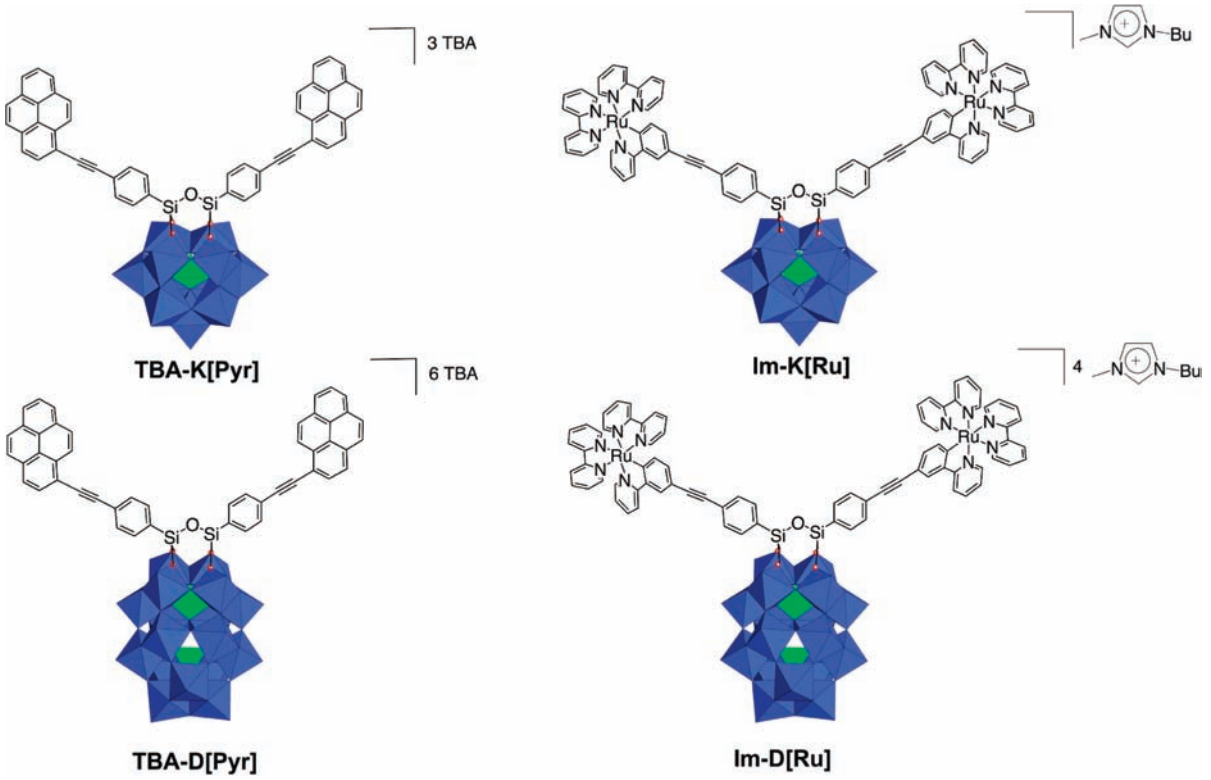

[a] TBA stands for tetrabutylammonium cation.

the isomers (Λ, Δ), (Λ, Λ), and (Δ, Δ). Combined 1D and 2D ^{1}H NMR experiments (see Supporting Information) and comparison with the ^{1}H spectra of the precursor allowed us to propose a full assignment of the ^{1}H resonances of **Im**−**K**[**Ru**] and **Im**−**D**[**Ru**] (Figure 1).

Electrochemistry. The redox properties of the pyrene-functionalized POMs **TBA**−**K**[**Pyr**] and **TBA**−**D**[**Pyr**] have been previously reported.[37] The new POM−ruthenium hybrids **Im**−**K**[**Ru**] and **Im**−**D**[**Ru**] and the reference compound **5** were investigated by cyclic voltammetry in deoxygenated DMF with $TBAPF_6$ as supporting electrolyte in a standard three-electrode cell, composed of a glassy carbon working electrode, a platinum counter electrode, and a saturated calomel reference electrode (SCE) (Table 1).

In the reduction part, **5** displays two reversible monoelectronic reduction processes assigned to the bipyridine units. In the oxidation part, the reversible redox process is attributed to the Ru(III)/Ru(II) couple. While the cyclic voltammograms of all the hybrids previously synthesized from the **TBA**−**K**[**I**] and **TBA**−**D**[**I**] plateforms were nicely resolved,[36,37] the cyclic voltammetry of **Im**−**K**[**Ru**] and **Im**−**D**[**Ru**] are slightly less defined (Figure 2). In particular, the peak-to-peak separations are more important in the POM−Ru systems, as evidenced in Table 1. This was attributed to the lower solubility of the POM−Ru hybrids in DMF and problems of adsorption at the working electrode. In particular for **Im**−**K**[**Ru**], an important adsorption was observed for potentials lower than −1.5 V vs SCE, precluding the observation of redox processes occurring below this potential.

For **Im**−**K**[**Ru**], the Ru(III)/Ru(II) couple appears at a slightly lower potential than for the reference compound **5** ($E_{1/2}$ = 0.57 and 0.59 V vs SCE, respectively). This difference is due to the electrostatic stabilization of the ruthenium by the polyanion. Similarly, the first two electron reductions of the POM appear at slightly more positive potentials for **Im**−**K**[**Ru**] than for **TBA**−**K**[**I**] or **TBA**−**K**[**Pyr**], in which the chromophore is neutral. The difference in half-wave potentials is more important for the second reduction of the POM than for the first one (90 and 10 mV, respectively). In the case of **Im**−**D**[**Ru**], the electrostatic effect is much more pronounced, due to the higher charge of the Dawson-type POM (6 versus 3 for the Keggin-type POM). The difference of the half-wave potential of the Ru(III)/Ru(II) couple between **Im**−**D**[**Ru**] and **5** is 140 mV, while the differences of the half-wave potentials of the POM/POM+1e, POM+1e/POM+2e, and POM+2e/POM+3e between **Im**−**D**[**Ru**] and **TBA**−**D**[**I**] are 200, 370, and 540 mV, respectively. The behavior of the Keggin **Im**−**K**[**Ru**] compared to that of the parent species, complex **5**, and **TBA**−**K**[**I**] and the comparison of **TBA**−**K**[**Pyr**]/**TBA**−**K**[**I**] and **TBA**−**D**[**Pyr**]/**TBA**−**D**[**I**] suggest a very weak electronic interaction between the ruthenium and pyrene chromophores and the polyanions (see also below unchanged spectral profiles for the chromophores). The larger shifts observed in the case of the Dawson **Im**−**D**[**Ru**] thus reflect its higher negative charge and predominant electrostatic effects, as noticed above.

Electronic Absorption and Photophysical Properties. The electronic absorption and luminescence spectra of all the compounds in DMF solutions at room temperature have been

dx.doi.org/10.1021/ic200906b |*Inorg. Chem.* 2011, 50, 7761–7768

Scheme 3. Molecular Drawing of the Ruthenium Complex Precursor 1

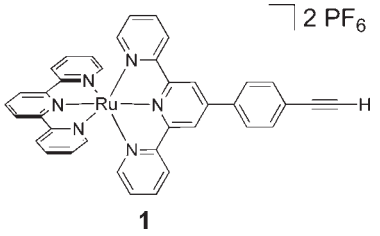

recorded, together with those of the ruthenium **5** and 1-ethynylpyrene models (Figure 3). The data are presented in Table 2.

The absorption spectrum of the ruthenium complex precursor **5** exhibits intense bands in the UV region due to $\pi-\pi^*$ ligand centered transitions and in the visible part of the spectrum attributed to metal to ligand charge transfer (MLCT) transitions. The two maxima at 490 and 538 nm are assigned to Ru→bpy (bpy = 2,2′-bipyridine) transitions, the latter one being highly red-shifted with respect to the one in $[Ru(bpy)_3]^{2+}$ because of the presence of the 3′-ethynyl-2-phenylpyridine ligand, which brings electronic density on the metal center as observed by electrochemistry and accordingly decreases the energy of the ruthenium to bipyridine transition. In agreement, the oxidation potential of **5** is lower than that of $[Ru(bpy)_3]^{2+}$ (1.28 V/SCE in MeCN).[38,41,48] Compound **5** displays a weak emission ($\phi = 1.3 \times 10^{-4}$) centered at 778 nm with a lifetime of 18.1 ns (see Table 2), attributed to deactivation of the lowest energy MLCT excited state. These low photophysical properties compared to those of $[Ru(bpy)_3]^{2+}$ (λ_{em} = 600 nm, ϕ = 0.062 in MeCN, τ = 890 ns)[48] can be rationalized by the energy gap law, since at low energy the coupling between excited and ground states is stronger and hence accelerates the nonradiative deactivations. The absorption spectra of compounds **Im**−**K**[**Ru**] and **Im**−**D**-[**Ru**] are dominated by the chromophore unit, since the POM itself does not contribute to the spectral profile in the visible region. In the hybrid Ru−POM systems the emission spectra shape and energy are roughly the same as those of the model chromophore **5**, whereas the lifetimes and quantum yields are reduced (see Table 2). The luminescence is partially quenched, most likely because of intramolecular oxidative electron transfer process occurring from the excited chromophore to the POM (a quenching mechanism by energy transfer can be ruled out because of the relative energies of both parts of the system). The driving force for such a process can be calculated by the Rehm−Weller equation (1):[49,50]

$$\Delta G = E_{ox}^* - E_{red} = (E_{ox} - E^{00}) - E_{red} \quad (1)$$

where E_{ox}^* is the oxidation potential of the excited chromophore, E^{00} the energy of the emitting excited state of the chromophore, and E_{red} the reduction potential of the electron acceptor subunit, i.e. of the POM. For **Im**−**K**[**Ru**] and **Im**−**D**-[**Ru**], the driving forces of the electron transfer processes are ∼−0.65 and −0.60 eV, respectively, the processes are thus thermodynamically allowed. The quenching rate constant k_q can be estimated by eq 2

$$k_q = 1/\tau - 1/\tau_0 \quad (2)$$

Scheme 4. Synthetic Route to the Ruthenium Complex Precursor 5[a]

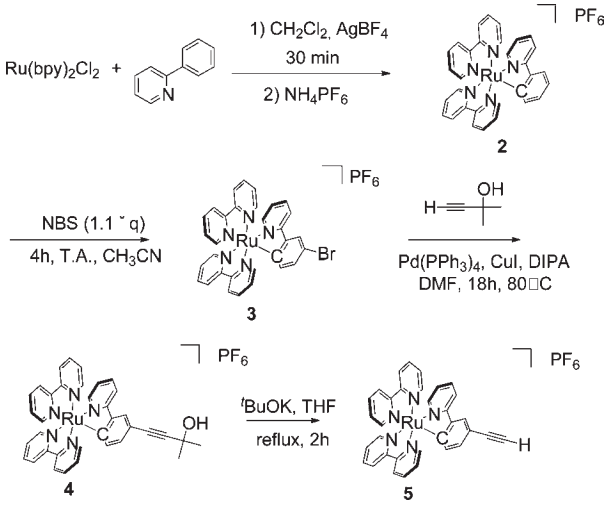

[a] DIPA stands for diisopropylamine.

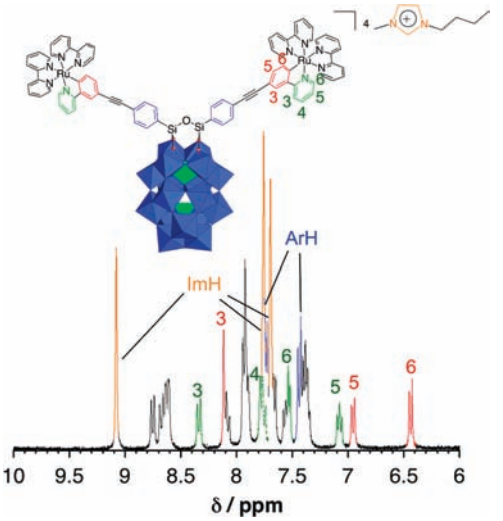

Figure 1. Enlargement of the 6−10 ppm region of the ^{1}H NMR (DMSO-d_6, 300 MHz) spectrum of **Im**−**D**[**Ru**].

where τ is the luminescence lifetime of the quenched species and τ_0 the lifetime of the model compound. The k_q values for **Im**−**K**[**Ru**] and **Im**−**D**[**Ru**] are 8×10^6 and 21×10^6 s^{-1}, respectively, relatively modest despite the favorable driving force of the process. This is attributed to the anionic cyclometalating ligand (C^N) that acts as a molecular insulator and delays the charge transfer to the POM. Indeed, in cyclometalated ruthenium(II) polypyridine complex, the LUMO is localized on the bypiridine units while the C^N π^* orbitals reside far above (0.7−1.4 eV in similar complexes).[51,52] In the POM−Ru system, the excited photoelectron would have to cross this energetic barrier to reduce the POM. Similarly, we could expect that the charge recombination would also be slow. However, for both hybrids no charge transfer state could be detected by nanosecond transient absorption spectroscopy.

dx.doi.org/10.1021/ic200906b |*Inorg. Chem.* 2011, 50, 7761–7768

Table 1. Half-Wave Potential (V vs SCE) and Peak-to-Peak Separation (mV) of the Redox Processes for the Reported Hybrids and Reference Compound ([a])

compound	P−1e/P	POM/POM+1e	POM+1e/POM+2e	POM+2e/POM+3e	P/P+1e	P+1e/P+2e
5	0.59 (85)				−1.46 (85)	−1.75 (85)
TBA−K[I]		−0.38 (75)	−0.97 (70)	−1.66 (155)		
TBA−D[I]		−0.73 (75)	−1.15 (70)	−1.74 (190)		
Im−K[Ru]	0.57 (160)	−0.37 (100)	−0.88 (150)			
Im−D[Ru]	0.45 (145)	−0.53 (130)	−0.78 (150)	−1.20 (90)	−1.51 (100)	
TBA−K[Pyr]	1.29 (irr)	−0.38 (70)	−0.97 (75)	−1.70 (nc)	−1.75 (95)	
TBA−D[Pyr]	1.29 (irr)	−0.73 (80)	−1.14 (75)	−1.75 (nc)	−1.75 (nc)	

[a] P refers to the photoactive antenna, nc = noncalculable.

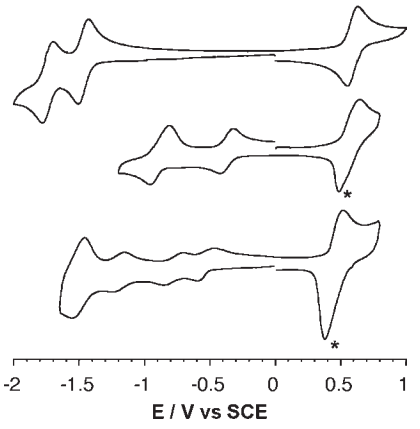

Figure 2. Cyclic voltammogram of 10^{-3} M solutions of **5** (top), **Im−K[Ru]** (middle), and **Im−D[Ru]** (bottom) in DMF containing 0.1 M of $TBAPF_6$. Scan rate: **5**, 200 mV s^{-1}; **Im−K[Ru]** and **Im−D[Ru]**, 400 mV s^{-1}. Working electrode, glassy carbon; reference electrode, SCE. The peaks noted with an asterisk correspond to adsorption processes of the hybrid on the working electrode.

This can be attributed either to a charge recombination rate faster than expected or to the very modest photophysical efficiency of the ruthenium chromophore that prevents significant charge transfer to the POM to proceed.

The absorption spectrum of the 1-ethynylpyrene is dominated by intense absorption bands (ε in the range 10^6−10^8 M^{-1} cm^{-1}) in the UV region, corresponding to π−π^* transitions.[50,53] The POM−pyrene hybrids exhibit absorption spectra with maxima extending to 390 nm. This value is close to the absorption maxima for arylethynylpyrenes derivatives (between 380 and 390 nm).[53] The 40 nm red-shift between the maximum absorption of the POM−pyrene and the 1-ethynylpyrene only reflects the increasing of the π-system when linking the POM hybrid to the 1-ethynylpyrene. The photophysical behavior of the pyrene-based species is similar to that of the Ru-based ones, i.e., a decrease of the emission properties of the pyrene is observed when linked to the polyoxometalate core (Table 2). The quenching process also in this case is likely an electron transfer from the pyrene moiety to the POM. From the redox and photophysical data, the driving force of such a process is $\Delta G \sim -1.45$ and −1.08 eV for **TBA−K[Pyr]** and **TBA−D[Pyr]**, respectively. The intramolecular quenching constant calculated from eq 2 is 3.3×10^8 and 3.6×10^8 s^{-1} for **TBA−K[Pyr]** and **TBA−D[Pyr]**, respectively. These values are much higher

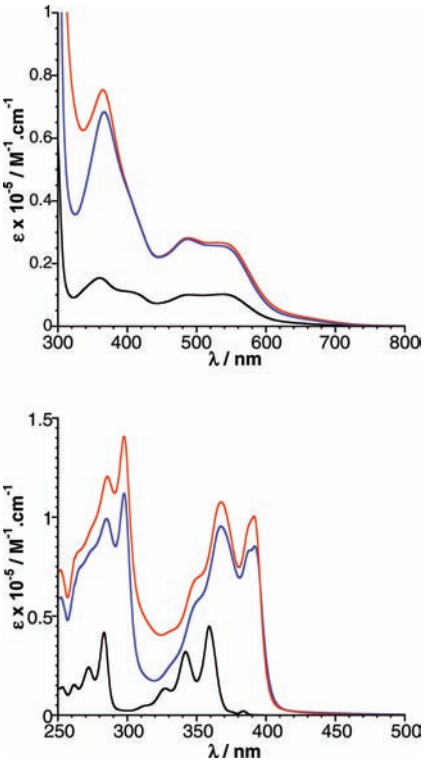

Figure 3. Absorption spectra recorded for the different hybrids and chromophore precursors in dilute DMF solution: (top) **5** (black), **Im−K[Ru]** (blue), **Im−D[Ru]** (red); (bottom) 1-ethynylpyrene (black), **Im−K[Pyr]** (blue), **TBA−D[Pyr]** (red).

than those of the POM−Ru system, reflecting the better thermodynamic parameter. Furthermore, no molecular insulator is present between the pyrene and the POM. No charge transfer state could be detected by nanosecond transient absorption spectroscopy, probably because of a fast charge recombination rate.

Covalent vs Electrostatic Hybrids. Lifetime measurement of the MLCT excited state of chromophore **5** was performed in the presence of the POM−based hybrid precursors **TBA−K[I]** and **TBA−D[I]** in deoxygenated DMF. In presence of the Keggin-type hybrid **TBA−K[I]**, in either 1:1 or 1:2 stoichiometry, the luminescence of **5** remains almost unchanged, the excited state having a lifetime of 18.0 ns. In presence of the Dawson-type hybrid **TBA−D[I]** in either 1:1 or 1:2 stoichiometry, a slight quenching of the luminescence is

dx.doi.org/10.1021/ic200906b |*Inorg. Chem.* 2011, 50, 7761–7768

Table 2. Electronic Absorption and Photophysical Data of the Compounds in Deaerated DMF Solutions at Room Temperature

compound	λ_{abs}, nm ($\varepsilon \times 10^{-3}$, M^{-1} cm^{-1})	λ_{em}, nm	τ, ns	ϕ
5	297 (63.7), 360 (15.4), 403 (11.1), 490 (10.1), 538 (10.2)	778	18.1	1.3×10^{-4}
Im−K[Ru]	368 (68.3), 485 (27.8), 539 (25.8)	780	15.8	0.6×10^{-4}
Im−D[Ru]	297 (271), 365 (75.5), 488 (28.2), 528 (26.7)	785	13.1	0.6×10^{-4}
1-ethynylpyrene	283 (41.7), 342 (32.0), 359 (44.8)	384	17.0[a]	0.65
TBA−K[Pyr]	298 (112), 367 (95.3), 391 (85.4)	398	2.6	0.003
TBA−D[Pyr]	298 (141), 368 (108), 391 (100)	401	2.4	0.0002

[a] From ref 47.

observed (τ = 17.0 ns). These results show that, as expected, the photoinduced electron transfer rate is faster in **Im−K[Ru]** and **Im−D[Ru]** covalent hybrids than in POM−ruthenium electrostatic adducts.

CONCLUSION

Postfunctionalization of hybrid disilylated POM platforms allowed us to prepare Keggin and Dawson-type polyoxometalates decorated by ruthenium and pyrene chromophores in a very efficient and modular way. Electrostatic interactions between negatively charged POMs and positively charged ruthenium complexes have been overcome by lowering the charge of the latter through the use of a phenylpyridine ligand. We thus provide an alternative to the electrostatic POM−Ru adducts until now described in the literature. As demonstrated by the quality of the ^{1}H and ^{31}P NMR spectra, we paid particular attention to the purification of the compounds, which is essential but not so easy in POM chemistry. Electronic properties have been inferred from electrochemical and photophysical studies and reflect poor electronic interactions between both partners. Quenching of the dye luminescence by electron transfer to the POMs is favored by its driving force, as calculated from the experimental data. In the case of the POM−Ru system, the lack of observation of a charge transfer state was attributed to the poor photophysical properties (low quantum yield and short-lived excited state) of the ruthenium complex. Still, the luminescence quenching of the ruthenium chromophore is more important in these covalent bonded hybrids than in systems where the POM and the ruthenium complexes are assembled via electrostatic interactions. The coupling of organometallic chromophores displaying efficient photophysical properties to the POM is currently under investigation.

EXPERIMENTAL SECTION

General. Reagents and solvents were obtained from commercial sources and used as received unless otherwise stated. $K_7[PW_{11}O_{39}]\cdot 14H_2O$ and $K_{10}[\alpha_2\text{-}P_2W_{17}O_{61}]\cdot 20H_2O$ were synthesized according to the literature procedure.[54,55] Microwave-assisted syntheses were performed in an ambient pressured reactor (Milestone Start S) equipped with a temperature control unit (operating conditions around 40 W). The ^{1}H (300.13 MHz), and $\{^{1}H\}^{31}P$ (121.5 MHz) NMR spectra were obtained at room temperature in 5 mm o.d. tubes on a Bruker AvanceII 300 spectrometer equipped with a QNP probehead. For ^{1}H, chemical shifts are referenced with respect to tetramethylsilane by using the solvent signals as secondary standard. For other nuclei, chemical shifts were measured by the substitution method and are given with respect to 85% H_3PO_4 (^{31}P). IR spectra were recorded from KBr pellets by using a Bio-Rad FT 165 spectrometer. The ESI mass spectra were recorded by using an on-trap mass spectrometer (Bruker Esquire 3000, Bremen, Germany) equipped with an orthogonal ESI source operated in the negative ion mode. The capillary high voltage was set to +3500 V. The capillary exit, skimmer 1, and skimmer 2 were typically set to −40, −10, and −6 V, respectively, in order to minimize insource decomposition. Sample solutions (10 pmol μL^{-1}) were infused into the ESI source by using a syringe pump at a flow rate of 120 $\mu L\ h^{-1}$. Elemental analysis was performed at the Institut des Substances Naturelles, Gif sur Yvette, France.

Photophysical Experiments. UV−visible spectra were recorded on an JASCO V-670 equipped with a ETC-717 Peltier module. Emission spectra were recorded in deoxygenated DMF solutions at room temperature on a Varian Cary Eclipse fluorescence spectrophotometer. Samples were placed in 1 cm path length quartz cuvettes. Luminescence lifetimes measurements were performed after irradiation at λ = 400 nm obtained by the second harmonic of a titanium:sapphire laser (picosecond Tsunami laser spectra physics 3950-M1BB + 39868-03 pulse picker doubler) at a 800 kHz repetition rate. Fluotime 200 from AMS technologies was used for the decay acquisition. It consists of a GaAs microchannel plate photomultiplier tube (Hamamatsu model R3809U-50) followed by a time-correlated single photon counting system from Picoquant (PicoHarp300). The ultimate time resolution of the system is close to 30 ps. Luminescence decays were analyzed with Fluofit software available from Picoquant. Emission quantum yields (ϕ) were determined at room temperature in acetonitrile solutions using the optically dilute method.[56]

$[Ru(bpy)_3]^{2+}$ (bpy = 2,2′-bipyridine) in air-equilibrated aqueous solution (ϕ = 0.028)[57] or pyrene in deoxygenated EtOH solution (ϕ = 0.53)[58] were used as quantum yield standard. Experimental uncertainties are as follows: emission maxima, 5 nm; emission lifetimes, 10%; emission quantum yields, 20%.

Synthesis of $[Ru(bpy)_2(ppH)]PF_6$ (2). The procedure was that described by Constable, except that the title compound was purified by chromatography instead of crystallization from MeOH.[59] Thus, under argon, a suspension of $[Ru(bpy)_2Cl_2]\cdot 2H_2O$ (1.5 g, 2.9 mmol) and 2-phenylpyridine (4.1 mL, 28.8 mmol) in CH_2Cl_2 (180 mL) is brought to reflux for 30 min, before adding $AgBF_4$ (1.12 g, 5.7 mmol).[60] The solution changed from violet to purple as a solid separated. After 2 h, the solution was filtered on diatomaceous earth, and the filtrate was concentrated in vacuum. To the oily residue was added a concentrated solution of NH_4PF_6 (1.4 g, 8.6 mmol) in MeOH (20 mL). Solvent was then partially removed under reduced pressure and complex **2** was precipitated with Et_2O. This operation was repeated until the excess of 2-phenylpyridine was removed. Complex **2** was then subjected to a chromatographic purification (alumina toluene/acetone). Yield 1.5 g (70%).

Synthesis of $[Ru(bpy)_2(ppBr)]PF_6$ (3). To a solution of **2** (1.0 g, 1.4 mmol) in CH_3CN (15 mL) was added a solution of *N*-bromosuccinimide (0.3 g, 1.7 mmol) in CH_3CN (10 mL) at room temperature. The red-purple solution turned to dark ruby red. The solution was stirred for 4 h. The reaction was quenched by addition of two drops of hydrazine hydrate, followed by ca. 200 mg of NH_4PF_6. After solvent removal, the product was purified by column chromatography (SiO_2, CH_2Cl_2). Yield:

dx.doi.org/10.1021/ic200906b |*Inorg. Chem.* 2011, 50, 7761–7768

1.1 g (95%). ^{1}H NMR (CD_3CN, 300 MHz): δ = 6.35 (d, J = 8.0 Hz, 1H), 6.93 (dd, J = 8.0 Hz, 2.1 Hz, 1H), 6.97 (td, J = 6.5 Hz, 1.4 Hz, 1H), 7.22 (td, J = 6.6 Hz, 1.3 Hz, 3H), 7.41 (td, J = 7.0 Hz, 1.2 Hz, 1H), 7.60 (dd J = 5.7 Hz, 1.3 Hz, 1H), 7.66−7.88 (m, 7H), 7.97−8.10 (m, 4H), 8.30 (dd, J = 8.0 Hz, 3.4 Hz, 2H), 8.39 (d, J = 8.0 Hz, 1H), 8.46 (d, J = 8.2 Hz, 1H). MS (FAB, NBA matrix): m/z = 638 $[M - PF_6 + H]^+$. Anal. Calcd for $C_{31}H_{23}N_5BrRuPF_6$: C, 47.07; H, 2.93; N, 8.85. Found: C, 46.94; H, 3.25; N, 8.66.

Synthesis of [Ru(bpy)$_2$(ppCC-C(Me)$_2$OH)]PF$_6$ (4). To a well-degassed (three cycles vacuum−argon) solution of **3** (500 mg, 0.63 mmol), $Pd(PPh_3)_4$ (30 mg, 0.03 mmol), and CuI (10 mg, 0.05 mmol) in DMF (4 mL) and diisopropylamine (1 mL) was added 2-methylbut-3-yn-2-ol (0.75 mL, 7.5 mmol), and the resulting mixture was stirred under argon at 80 °C for 18 h. Solvents were then stripped off under high vacuum. The crude material was dissolved in a minimum amount of CH_3CN and then excess NH_4PF_6 was added (ca. 30 mg). After evaporation to dryness crude material was taken in CH_2Cl_2 and applied on a chromatography column (SiO_2, CH_2Cl_2). Starting material was eluted first with pure CH_2Cl_2 and then the title compound with CH_2Cl_2:MeOH 9.8:0.2. After evaporation the compound was redissolved in acetone and precipitated with Et_2O to yield the pure compound as a bright dark red lacquer. Yield: 400 mg (80%). ^{1}H NMR (CD_3CN, 300 MHz): δ = 8.46 (d, J = 8.2 Hz, 1H), 8.38 (d, J = 7.9 Hz, 1H), 8.30−8.35 (m, 2H), 7.96−8.07 (m, 3H), 7.68−7.87 (m, 8H), 7.58 (dd, J = 5.6 Hz, 1 Hz, 1H), 7.42 (ddd, J = 7.7 Hz, 5.6 Hz, 1.2 Hz, 1H), 7.18−7.25 (m, 3H), 6.96 (td, J = 6.7 Hz, 1.3 Hz, 1H), 6.82 (dd, J = 7.7 Hz, 1.7 Hz, 1H), 6.44 (d, J = 7.7 Hz, 1H), 1.50 (s, 6H). MS (FAB, NBA matrix): m/z = 650 $[M - PF_6]^+$. Anal. Calcd for $C_{36}H_{30}N_5ORuPF_6 \cdot 1.3Et_2O$ (%): C, 55.53; H, 4.86; N, 7.86. Found: C, 55.17; H, 5.15; N, 7.89 (presence of diethyl ether confirmed by ^{1}H NMR).

Synthesis of [Ru(bpy)$_2$(ppCC-H)]PF$_6$ (5). A solution of **4** (150 mg, 0.19 mmol) and ^{t}BuOK (25 mg, 0.22 mmol) in degassed THF (5 mL) was refluxed for 2 h. The reaction was monitored by TLC (SiO_2, CH_2Cl_2:MeOH 9.8:0.2) until disappearance of the slow-moving starting alcohol compound. The deprotection is essentially quantitative. Solvent was then removed in vacuum, crude material was then retaken in CH_2Cl_2, and insolubles were filtered off. After evaporation the compound is used without further purification. If needed, it can be further purified by column chromatography (SiO_2, CH_2Cl_2).^{1}H NMR (CD_3CN, 300 MHz): δ = 8.46 (d, J = 8.1 Hz, 1H), 8.40 (d, J = 8.1 Hz, 1H), 8.33 (dd, J = 8.0 Hz, 3.0 Hz, 2H), 7.96−8.08 (m, 4H), 7.69−7.87 (m, 7H), 7.61 (dd, J = 4.0 Hz, 1.0 Hz, 1H), 7.43 (td, J = 7.0 Hz, 1.2 Hz, 1H), 7.18−7.26 (m, 3H), 6.98 (dd, J = 7.7 Hz, 1.6 Hz, 1H), 6.92 (td, J = 6.0 Hz, 1.4 Hz, 1H), 6.50 (d, J = 7.8 Hz, 1H), 3.26 (s, 1H). MS (FAB, NBA matrix) m/z: 592 $[M - PF_6 + H]^+$.

Synthesis of Im−D[Ru]. **TBA−D[I]** (140 mg, 0.023 mmol, 1 equiv), **5** (43 mg, 0.058 mmol, 2.5 equiv), $Pd(PPh_3)_2Cl_2$ (0.0023 mmol, 10 mol %), and CuI (0.0035 mmol, 15 mol %) were dissolved in 5 mL of dried and freshly distilled DMF. After careful degassing with argon for 10 min, freshly distilled Et_3N (0.46 mmol, 20 equiv) was added. The mixture was stirred at 70 °C for 1 h under microwave irradiation. After cooling to room temperature, TBABr (148 mg, 20 equiv) was added to the mixture which was then precipitated with Et_2O to separate the crude by filtration. The solid was dissolved in a minimum amount of DMSO and 3 mL of 1-butyl-3-methylimidazolium chloride was added under stirring to perform the metathesis. The resulting solution was precipitated with EtOH, filtrated, and washed with EtOH and Et_2O to obtain **Im−D[Ru]** as a dark red-purple powder. Yield: 121 mg (86%). ^{1}H NMR (DMSO-d_6, 300 MHz): δ = 9.09 (s, 4H), 8.66 (d, 2H), 8.61−8.64 (m, 6H), 8.35 (d, 2H), 8.09 (m, 4H), 7.93 (m, 8H), 7.65−7.79 (m, 20H), 7.54 (m, 4H), 7.37−7.46 (m, 10H), 7.08 (t, 2H), 6.96 (d, 2H), 6.44 (d, 2H), 4.18 (t, 8H), 3.87 (s, 12H), 1.77 (m, 8H), 1.26 (m, 8H), 0.89 (t, 12H). ^{31}P NMR (DMSO-d_6): δ = −10.78 and −13.78 ppm. MS (ESI): most intense peaks, $\{aggregates\}^{x-}$ m/z (%): $\{D[Ru]\}^{4+}$ 1392.6 (100), calcd 1392.3; $\{Im-D[Ru]\}^{3-}$ 1902.3 (60), calcd 1902.0. IR (KBr, cm^{-1}): ν = 2194 (vw), 1626 (w), 1598 (w), 1577(w), 1461 (w), 1443 (w), 1421 (w), 1262 (w), 1165 (w), 1089 (m), 1039 (w), 954 (s), 919 (s), 811 (s), 762 (s), 731 (sh), 530 (m), 390 (m). Anal. Calcd for $P_2W_{17}O_{62}Si_2Ru_2C_{110}H_{114}N_{18}$ (%): C, 21.57; H, 1.88; N, 4.12. Found: C, 22.05; H, 1.85; N, 4.09.

Synthesis of Im−K[Ru]. Compound **Im−K[Ru]** was prepared analogously. It was isolated as a dark red-purple powder. Yield: 64 mg (76%). ^{1}H NMR (DMSO-d_6): δ = 9.10 (s, 1H), 8.76 (d, 2H), 8.62−8.70 (m, 6H), 8.33 (d, 2H), 8.09 (m, 4H), 7.93 (m, 8H), 7.57−7.76 (m, 14H), 7.54 (m, 4H), 7.35−7.43 (m, 10H), 7.10 (t, 2H), 6.96 (d, 2H), 6.45 (d, 2H), 4.16 (t, 2H), 3.85 (s, 3H), 1.75 (m, 2H), 1.26 (m, 2H), 0.90 (t, 3H). ^{31}P NMR (DMSO-d_6): δ = −13.53 ppm. IR (KBr, cm^{-1}): ν = 2197 (vw), 1654 (vw), 1598 (w), 1578 (w), 1461 (w), 1443 (w), 1420 (w), 1261 (w), 1163 (w), 1110 (m), 1058 (sh), 1039 (w), 1016 (sh), 965 (s), 870 (s), 822 (s), 761 (s), 730 (sh), 521 (m), 391 (m). Anal. Calcd for $PW_{11}O_{40}Si_2Ru_2C_{86}H_{69}N_{12}$ (%): C, 24.46; H, 1.65; N, 3.98. Found: C, 24.60; H, 1.77; N, 4.00.

■ ASSOCIATED CONTENT

Supporting Information. ^{1}H NMR spectrum of compound **5**, ^{1}H and ^{31}P NMR spectra of compounds **Im−K[Ru]** and **Im−D[Ru]**, and ^{1}H COSY NMR spectrum of compound **Im−D[Ru]**. This material is available free of charge via the Internet at http://pubs.acs.org.

■ AUTHOR INFORMATION

Corresponding Author
*E-mail: guillaume.izzet@upmc.fr.

■ ACKNOWLEDGMENT

Sandrine Fraysse is greatly acknowledged for participating in the synthesis of compound **5**. F.L. thanks the chemistry platform (Nanobio Campus) in Grenoble for use of the luminescent lifetime measurement facilities.

■ REFERENCES

(1) Oneil, M. P.; Niemczyk, M. P.; Svec, W. A.; Gosztola, D.; Gaines, G. L.; Wasielewski, M. R. *Science* **1992**, *257*, 63–65.
(2) Konduri, R.; Ye, H. W.; MacDonnell, F. M.; Serroni, S.; Campagna, S.; Rajeshwar, K. *Angew. Chem., Int. Ed.* **2002**, *41*, 3185–3187.
(3) Baffert, C.; Artero, V.; Fontecave, M. *Inorg. Chem.* **2007**, *46*, 1817–1824.
(4) Jacques, P. A.; Artero, V.; Pecaut, J.; Fontecave, M. *Proc. Natl. Acad. Sci. U. S. A.* **2009**, *106*, 20627–20632.
(5) Artero, V.; Fontecave, M. *Coord. Chem. Rev.* **2005**, *249*, 1518–1535.
(6) Wilson, A. D.; Shoemaker, R. K.; Miedaner, A.; Muckerman, J. T.; DuBois, D. L.; DuBois, M. R. *Proc. Natl. Acad. Sci. U. S. A.* **2007**, *104*, 6951–6956.
(7) Wilson, A. D.; Newell, R. H.; McNevin, M. J.; Muckerman, J. T.; DuBois, M. R.; DuBois, D. L. *J. Am. Chem. Soc.* **2006**, *128*, 358–366.
(8) Brewer, K. J.; Arachchige, S. M.; Brown, J. R.; Chang, E.; Jain, A.; Zigler, D. F.; Rangan, K. *Inorg. Chem.* **2009**, *48*, 1989–2000.
(9) Odobel, F.; Karlsson, S.; Boixel, J.; Pellegrin, Y.; Blart, E.; Becker, H. C.; Hammarstrom, L. *J. Am. Chem. Soc.* **2010**, *132*, 17977–17979.
(10) Proust, A.; Thouvenot, R.; Gouzerh, P. *Chem. Commun.* **2008**, 1837–1852.
(11) Dolbecq, A.; Dumas, E.; Mayer, C. R.; Mialane, P. *Chem. Rev.* **2010**, *110*, 6009–6048.

(12) Pope, M. T. In *Comprehensive Coordination Chemistry II*; McCleverty, J., Meyer, T. J., Eds.; Elsevier: Oxford, 2004; Vol. 4, pp 635−678.
(13) Hill, C. L. *Chem. Rev.* **1998**, *98*, 1-390 (special issue devoted to polyoxometalates).
(14) Sadakane, M.; Steckhan, E. *Chem. Rev.* **1998**, *98*, 219–237.
(15) Keita, B.; Nadjo, L. *J. Mol. Catal. A: Chem.* **2007**, *262*, 190–215.
(16) Keita, B.; Kortz, U.; Holzle, L. R. B.; Brown, S.; Nadjo, L. *Langmuir* **2007**, *23*, 9531–9534.
(17) Papaconstantinou, E. *Chem. Soc. Rev.* **1989**, *18*, 1–31.
(18) Troupis, A.; Gkika, E.; Triantis, T.; Hiskia, A.; Papaconstantinou, E. *J. Photochem. Photobiol., A* **2007**, *188*, 272–278.
(19) Hill, C. L.; Bouchard, D. A.; Kadkhodayan, M.; Williamson, M. M.; Schmidt, J. A.; Hilinski, E. F. *J. Am. Chem. Soc.* **1988**, *110*, 5471–5479.
(20) Renneke, R. F.; Pasquali, M.; Hill, C. L. *J. Am. Chem. Soc.* **1990**, *112*, 6585–6594.
(21) Duncan, D. C.; Netzel, T. L.; Hill, C. L. *Inorg. Chem.* **1995**, *34*, 4640–4646.
(22) Ruther, T.; Hultgren, V. M.; Timko, B. P.; Bond, A. M.; Jackson, W. R.; Wedd, A. G. *J. Am. Chem. Soc.* **2003**, *125*, 10133–10143.
(23) Yamase, T.; Cao, X. O.; Yazaki, S. *J. Mol. Catal. A: Chem.* **2007**, *262*, 119–127.
(24) Schaming, D.; Costa-Coquelard, C.; Sorgues, S.; Ruhlmann, L.; Lampre, I. *Appl. Catal., A* **2010**, *373*, 160–167.
(25) Song, J.; Luo, Z.; Zhu, H.; Huang, Z.; Lian, T.; Kaledin, A. L.; Musaev, D. G.; Lense, S.; Hardcastle, K. I.; Hill, C. L. *Inorg. Chim. Acta* **2010**, *363*, 4381–4386.
(26) Xie, J. L.; Abrahams, B. F.; Wedd, A. G. *Chem. Commun.* **2008**, 576–578.
(27) Fay, N.; Hultgren, V. M.; Wedd, A. G.; Keyes, T. E.; Forster, R. J.; Leane, D.; Bond, A. M. *Dalton Trans.* **2006**, 4218–4227.
(28) Keyes, T. E.; Gicquel, E.; Guerin, L.; Forster, R. J.; Hultgren, V.; Bond, A. M.; Wedd, A. G. *Inorg. Chem.* **2003**, *42*, 7897–7905.
(29) Wang, X. L.; Han, Z. B.; Wang, E. B.; Zhang, H.; Hu, C. W. *Electroanalysis* **2003**, *15*, 1460–1464.
(30) Kang, J.; Xu, B. B.; Peng, Z. H.; Zhu, X. D.; Wei, Y. G.; Powell, D. R. *Angew. Chem., Int. Ed.* **2005**, *44*, 6902–6905.
(31) Schaming, D.; Costa-Coquelard, C.; Lampre, I.; Sorgues, S.; Erard, M.; Liu, X.; Liu, J.; Sun, L.; Canny, J.; Thouvenot, R.; Ruhlmann, L. *Inorg. Chim. Acta* **2010**, *363*, 2185–2192.
(32) Allain, C.; Favette, S.; Chamoreau, L. M.; Vaissermann, J.; Ruhlmann, L.; Hasenknopf, B. *Eur. J. Inorg. Chem.* **2008**, 3433–3441.
(33) Harriman, A.; Elliott, K. J.; Alamiry, M. A. H.; Le Pleux, L.; Severac, M.; Pellegrin, Y.; Blart, E.; Fosse, C.; Cannizzo, C.; Mayer, C. R.; Odobel, F. *J. Phys. Chem. C* **2009**, *113*, 5834–5842.
(34) Odobel, F.; Severac, M.; Pellegrin, Y.; Blart, E.; Fosse, C.; Cannizzo, C.; Mayer, C. R.; Eliott, K. J.; Harriman, A. *Chem.—Eur. J.* **2009**, *15*, 3130–3138.
(35) Elliott, K. J.; Harriman, A.; Le Pleux, L.; Pellegrin, Y.; Blart, E.; Mayer, C. R.; Odobel, F. *Phys. Chem. Chem. Phys.* **2009**, *11*, 8767–8773.
(36) Duffort, V.; Thouvenot, R.; Afonso, C.; Izzet, G.; Proust, A. *Chem. Commun.* **2009**, 6062–6064.
(37) Matt, B.; Renaudineau, S.; Chamoreau, L. M.; Afonso, C.; Izzet, G.; Proust, A. *J. Org. Chem.* **2011**, *76*, 3107–3112.
(38) Juris, A.; Balzani, V.; Barigelletti, F.; Campagna, S.; Belser, P.; Vonzelewsky, A. *Coord. Chem. Rev.* **1988**, *84*, 85–277.
(39) Sauvage, J. P.; Collin, J. P.; Chambron, J. C.; Guillerez, S.; Coudret, C.; Balzani, V.; Barigelletti, F.; Decola, L.; Flamigni, L. *Chem. Rev.* **1994**, *94*, 993–1019.
(40) Balzani, V.; Juris, A.; Venturi, M.; Campagna, S.; Serroni, S. *Chem. Rev.* **1996**, *96*, 759–833.
(41) Alstrum-Acevedo, J. H.; Brennaman, M. K.; Meyer, T. J. *Inorg. Chem.* **2005**, *44*, 6802–6827.
(42) Constable, E. C.; Housecroft, C. E.; Johnston, L. A.; Armspach, D.; Neuburger, M.; Zehnder, M. *Polyhedron* **2001**, *20*, 483–492.
(43) Coudret, C.; Fraysse, S.; Launay, J. P. *Chem. Commun.* **1998**, 663–664.
(44) Fraysse, S.; Coudret, C.; Launay, J. P. *J. Am. Chem. Soc.* **2003**, *125*, 5880–5888.
(45) Wasserscheid, P.; Keim, W. *Angew. Chem., Int. Ed.* **2000**, *39*, 3772–3789.
(46) Zhang, J.; Bond, A. M.; MacFarlane, D. R.; Forsyth, S. A.; Pringle, J. M.; Mariotti, A. W. A.; Glowinski, A. F.; Wedd, A. G. *Inorg. Chem.* **2005**, *44*, 5123–5132.
(47) Coleman, A.; Pryce, M. T. *Inorg. Chem.* **2008**, *47*, 10980–10990.
(48) Shan, B. Z.; Zhao, Q.; Goswami, N.; Eichhorn, D. M.; Rillema, D. P. *Coord. Chem. Rev.* **2001**, *211*, 117–144.
(49) Rehm, D.; Weller, A. *Ber. Bunsen-Ges. Phys. Chem.* **1969**, *73*, 834–839.
(50) Rehm, D.; Weller, A. *Isr. J. Chem.* **1970**, *8*, 259–271.
(51) Pfeffer, M.; Djukic, J. P.; Sortais, J. B.; Barloy, L. *Eur. J. Inorg. Chem.* **2009**, 817–853.
(52) Berlinguette, C. P.; Bomben, P. G.; Koivisto, B. D. *Inorg. Chem.* **2010**, *49*, 4960–4971.
(53) Yang, S. W.; Elangovan, A.; Hwang, K. C.; Ho, T. I. *J. Phys. Chem. B* **2005**, *109*, 16628–16635.
(54) Souchay, P. *Polyanions et Polycations*; Gauthier-Villars: Paris, 1963.
(55) Contant, R. *Inorg. Synth.* **1990**, *27*, 104–111.
(56) Demas, J. N.; Crosby, G. A. *J. Phys. Chem.* **1971**, *75*, 991–1024.
(57) Nakamaru, K. *Bull. Chem. Soc. Jpn.* **1982**, *55*, 2697–2705.
(58) Dawson, W. R.; Windsor, M. W. *J. Phys. Chem.* **1968**, *72*, 3251–3260.
(59) Constable, E. C.; Holmes, J. M. *J. Organomet. Chem.* **1986**, *301*, 203–208.
(60) Viala, C.; Coudret, C. *Inorg. Chim. Acta* **2006**, *359*, 984–989.